Omnidirectional Static Walking of a Quadruped Robot

Shugen Ma, *Member, IEEE*, Takashi Tomiyama, and Hideyuki Wada

***Abstract*—In this paper, we propose a successive gait-transition method for a quadruped robot to realize omnidirectional static walking. The gait transition is successively performed among the crawl gaits and the rotation gaits, while the feet hold in common positions before and after gait transition. The gait-transition time is reduced by carefully designing the foot positions of the crawl gait and the rotation gait, while limiting the feet in rectangular reachable motion ranges. Computer simulations and experiments were executed to show the validity and the limitation of the proposed gait-transition method.**

***Index Terms*—Crawl gait, omnidirectional walking, quadruped robot, rotation gait, static walking, successive gait transition.**

I. Introduction

THE legged robot was expected to be an environment-accessible platform because of its environmental adaptability. With consideration of stability and energy consumption, the quadruped walking robot will be one of the most practical locomotion machines to move about on uneven terrain, and is stablest while walking in a static state [1]. Studies of quadruped gaits can be divided in two parts, according to the nature of the stability, static stability or dynamic stability. Static stability assumes that the vertical projection of the center of gravity (COG) remains always inside the stability polygon with an adequate stability margin during all phases of movements. The stability margin ensures that whatever speed the robot can reach, it will not be carried away by its own momentum, and consequently tip over and fall down. In this paper, we focus on the static walking of a quadruped robot for its static stability. This is important for considering the carriage of heavy goods.

One type of static walking gait, named the crawl gait, was introduced by McGhee [2] and appears to be very close to the walk frequently used by mammals at low speed [3]. For the robot to perform the movement in any decided direction, Hirose extended the crawl gait to a standard side-walking gait, the crab gait [4]. We classify this crab gait to crawl gait in this paper. Moreover, for the quadruped robot to perform a rotation, a rotation gait was introduced [5] that gives the maximum rotation velocity around any center of turning. To manage the transition between the "standing postures," which represent the position and attitude of the platform, the moving speed, and the supporting patterns of all four legs, the standing-posture transformation gait was proposed [6]. This algorithm connects the walking gaits with a static convergence leg position and has the torso stop in at least four steps. Using this algorithm, the robot cannot perform an omnidirectional static walk with the least time of torso stop. Recently, the semiautonomous walking of a quadruped robot, based on leg transition at the border of the leg work space, has been proposed [7], and the gait transitions between forward, backward, left, and right turning and rotation motions have been discussed in cooperation with sideways motion of the torso [8]. In previous papers, the omnidirectional static walk has not been perfectly performed. For the purpose of RoboCup competitions, Bruce *et al.* proposed fast parametric transitions to smooth quadruped motion [9]. However, their proposed algorithm does not deal with gait transition between different gaits. To solve the previous problems, we realize the omnidirectional static walk of the quadruped robot without sideways motion of the torso for better efficiency in energy consumption. The discussed omnidirectional static walk is not only performing a given direction walk, such as crab walking, but also performing the successive walk while the walking direction and the walking speed are changed. The walking-gait planning technique chooses the crawl gait or rotation gait from the center of turning, and transfers the gaits from one to another continuously when changing the center of turning.

The rest of this paper is organized as follows. Section II briefly introduces the procedure to realize the omnidirectional static walk of the quadruped robot. Section III gives the planning technique of the crawl gait with an arbitrary turning center and the rotation gaits that are the standard gaits of omnidirectional static walking, where the feet before and after gait transition are designed to have common positions to perform the gait transition with the fewest steps. Section IV proposes the successive gait-transition procedures while changing the turning center, with the assumption that the gait transition is executed at one step before the diagonal triangle exchange (DTE) point [10]. Simulations and experiments were performed to show the validity of the proposed omnidirectional static walking method, and their results are presented in Section V. Finally, Section VI gives the conclusions of the paper.

II. Omnidirectional Static Walking Gaits

As mentioned in the Introduction, the most basic static walking pattern for the quadruped robot is the crawl gait (in-

Manuscript received May 21, 2003; revised November 17, 2003. This paper was recommended for publication by Associate Editor Y. H. Liu and Editor I. Walker upon evaluation of the reviewers' comments. this paper was presented in part at the IEEE/RSJ International Conference on Intelligent Robots and Systems, Lausanne, Switzerland, September 30–October 4, 2002.

S. Ma is with the Department of Systems Engineering, Faculty of Engineering, Ibaraki University, Ibaraki-Ken 316-8511, Japan. He is also with the Shenyang Institute of Automation, Chinese Academy of Sciences, Shenyang, China (e-mail: shugen@dse.ibaraki.ac.jp).

T. Tomiyama is with Toshiba Tec Corp., Tokyo 101-8442, Japan (e-mail: Takashi_Tomiyama@toshibatec.co.jp).

H. Wada is with System Technology Corp., Tokyo 101-8442, Japan.

Digital Object Identifier 10.1109/TRO.2004.835448

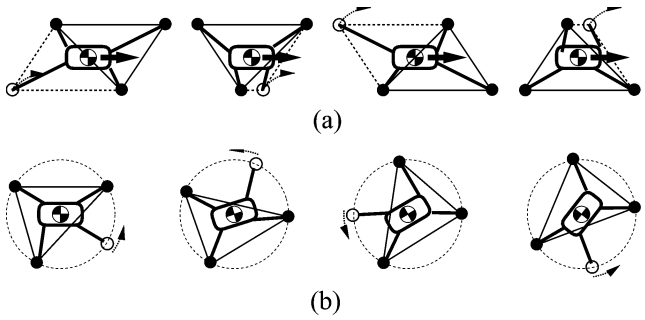

Fig. 1. Crawl gait and rotation gait. (a) Crawl gait. (b) Rotation gait.

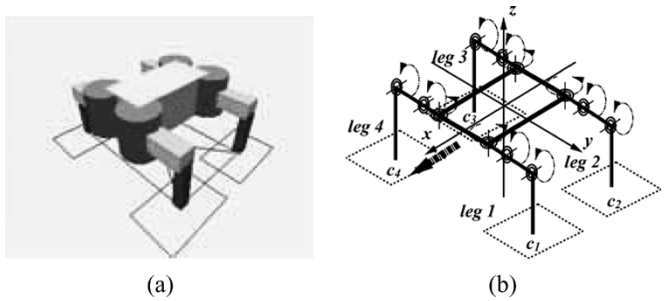

Fig. 2. Robot model and coordinate located on the robot. (a) Robot model. (b) Coordinate.

cluding crab gait), as shown in Fig. 1(a). This gait is not only for straight-line movement but also for a curve movement with small curvature. While the curvature becomes larger or the center of turning is near the COG, the rotation gait shown in Fig. 1(b) has better static stability and higher motion speed than the crawl gait. The successive omnidirectional static walking is generated by continuous gait transition between these crawl and rotation gaits. In this paper, we first introduce the planning technique of the standard gaits (crawl gait and rotation gait) that is more convenient for gait transition, and then discuss the successive gait transition between any crawl gaits and any rotation gaits. The omnidirectional static walking of the quadruped robot can be realized by the following procedures.

Standard gait planning: After selecting the gait from the turning center, plan the leg positions and trajectories with constraints of the legs' reachable range.

1) Select a gait from the position of the turning center.
2) Derive the landing position of the swinging leg and the lifting position of the supporting leg from the motion speed while limiting the legs within their reachable range.
3) Plan the leg trajectories that connect corresponding points.

Successive gait-transition: Transfer gait successively, corresponding to the change of the turning center.

1) Select the next gait and derive the next-step legs' positions from the new position of the turning center.
2) Move the legs from the current legs' positions to the new legs' positions successively, while the feet hold in common positions before and after gait transition.

In this paper, we use the robot model shown in Fig. 2(a) and set the torso coordinate as in Fig. 2(b). The origin of the coordinate is located at the COG, with its x axis in the back-to-front direction of the torso, its y axis in the right-to-left direction, and its z axis in the bottom-to-top direction. The legs are labeled 1 to 4, as shown in Fig. 2. Assume the robot posture shown in Fig. 2 to be the basic posture, and the corresponding legs' positions as the legs' basic positions. While walking, the robot is assumed to control its posture so as to keep the torso horizontally in the height of the COG, c_{iz}. Then, the problem of assigning the leg motions becomes a planar one, and we can consider the work space of each leg to be defined by a planar area (a rectangle in this paper, for simplicity) corresponding to that fixed height, c_{iz}. The supporting leg's motion and the swinging leg's motion are both planned in the coordinate fixed on the robot torso. The duty factor β is assumed to be 0.75 for the crawl gait where the motion speed of the robot is adjusted through changing the stroke of legs and their swinging speed. The time of swinging leg $T_{\rm sw}$ is fixed to a constant value.

III. Planning Standard Gaits

In this section, we give the planning technique of the crawl gait with an arbitrary turning center and the rotation gait that are the standard gaits of omnidirectional static walking. These standard gaits are for possibly transferring the gaits continuously. In order to perform the gait transition with the fewest steps, the feet before and after gait transition are designed to have common positions, as shown in Fig. 3. The positions of the supporting legs at the basic posture are defined as the common positions of the standard gaits. The standard gaits discussed in this paper are different from the rotation gait [5] that always uses the maximum rotation velocity around any center of turning, since they can choose any rotation speed within its limit and be planned with consideration of successive gait transition. The successive gait transition based on the discussed standard gaits can also be used for starting phase from the basic posture and ending phase to the basic posture without any change. The planning method of the crawl gait and that of the rotation gait are almost the same, except for the position of the turning center and the sequence of leg swinging. The standard gaits are planned through: 1) selecting a gait pattern from the position of the turning center; 2) deriving the landing position of a swinging leg and the lifting positions of the supporting legs; and 3) planning the leg trajectories that connect corresponding points.

A. Selection of Gait Pattern

We assume that the walking speed and rotation speed are given by an operator or from navigation.

In this section, we first derive the radius of the turning curve, r_g, and the position of the turning center, $\boldsymbol{Q}$, from the given walking speed, $\boldsymbol{v}_{in}$, and the rotation speed, $\dot{\theta}_{in}$. The radius of the turning curve r_g can be given by

$$r_g = \frac{|\boldsymbol{v}_{in}|}{|\dot{\theta}_{in}|}. \tag{1}$$

If the rotation speed $\dot{\theta}_{in}$ is zero (in the case of straight-line walking), we use a small value instead (in simulations and ex-

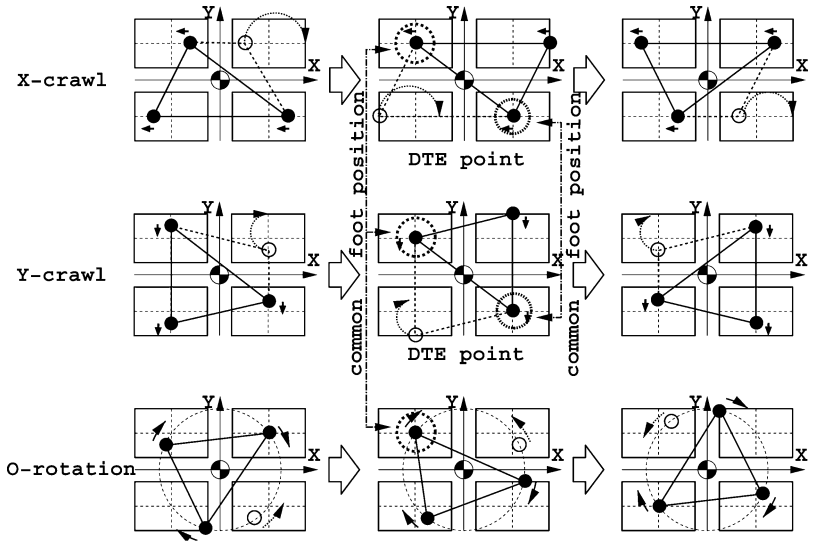

Fig. 3. Common foot position for each walking gait.

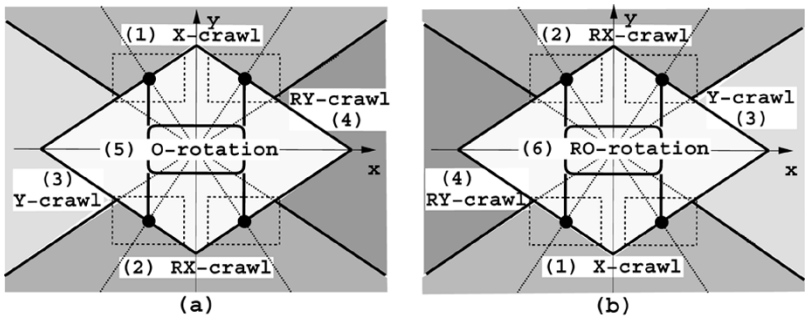

Fig. 4. Gait selection by center of curvature. (a) Left turn. (b) Right turn.

periments, 10^{-10} was used). The position of the turning center, $\boldsymbol{Q}$, located at the ground, can be described by

$$\boldsymbol{Q} = \mathbf{Rot}\left(\boldsymbol{k}, \frac{\pi}{2}\right)\begin{bmatrix}\boldsymbol{v}_{in} \\ \dot{\theta}_{in}\end{bmatrix} - c_{iz}\Bigg]^{T} \tag{2}$$

where $\mathbf{Rot}(\boldsymbol{k}, \pi/\mathbf{2})$ is the rotation matrix that rotates a $\pi/2$ angle around the z axis.

Next, we select the walking-gait pattern from the above-derived position of the turning center. Through mapping the position of the turning center and the turning direction onto Fig. 4, the walking-gait pattern that should be used can be selected from Fig. 5. For example, if the robot turns counterclockwise and the position of the turning center is on the (5) area of Fig. 4(a), the robot consequently selects the walking-gait pattern (5) of Fig. 5.

It should be pointed out that the rotation gait is selected in the case that the walking speed and the rotation speed are zero (the robot is stopped). As a result, the starting phase from the basic posture can be seen as the gait transition from the rotation gait, and the ending phase to the basic posture can be seen as the gait transition to the rotation gait. That is, the walking from start to the limit speed (or from the limit speed to end) can be seen as the gait transition from (or to) the rotation gait.

Fig. 4, showing the region for gait selection by the center of curvature, is obtained from the relation between the position of the turning center and the stability margin while using the rotation gait, and from the critical angle between the X-crawl gait and the Y-crawl gait. Since there is no DTE point in the rotation gait, the robot can always walk with a positive stability margin while the turning center is near the center of the torso. Thus, the rotation gait is preferably used in the case where the turning

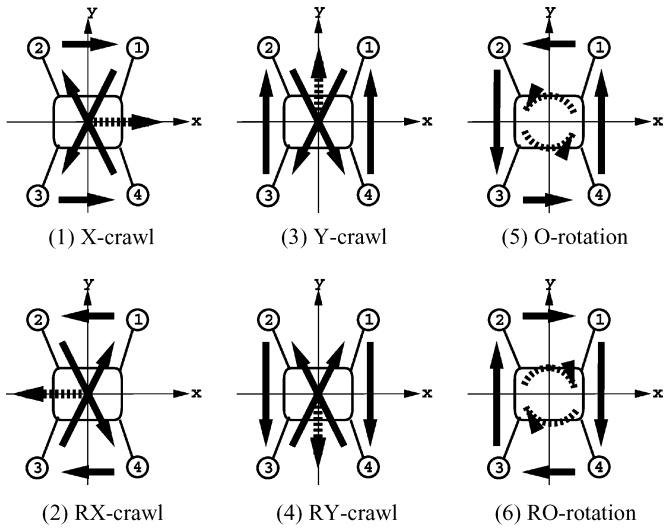

Fig. 5. Each type of static walking gait. (1) X-crawl. (2) RX-crawl. (3) Y-crawl. (4) RY-crawl. (5) O-rotation. (6) RO-rotation.

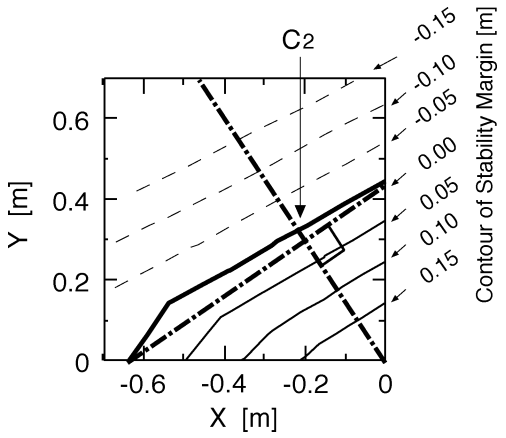

Fig. 6. Contour of stability margin for rotation gait.

center is near the center of the torso. The boundary for clarifying the use of the rotation gait and the crawl gait is not quite clear. We here derive the border, where the stability margin of the rotation gait is zero, by computer simulation. In the computer simulation, the parameters of the robot model mentioned in Section V were used, and the rotation speed was set to 0.06 rad/s. As the robot model is symmetric in fore–aft and right–left directions, we only show the obtained contour of the stability margin of the second phase in Fig. 6. From this result, we know that:

- the border of zero stability margin is almost a straight line;
- the stability margin is the inverse proportion of the distance of the turning center from the COG;
- the stability margin decreases in highest speed along the line that connects the origin of the torso coordinate and the leg's basic position.

The boundary for clarifying the use of the rotation gait, thus, can be approximately given by a line

$$y = -\frac{c_{ix}}{c_{iy}}x + \frac{c_{ix}^2 + c_{iy}^2}{c_{iy}}. \tag{3}$$

This line is passing through the leg's basic position $\boldsymbol{c}_i$ and normal to the line that connects the origin of the torso coordinate and the leg's basic position. The line obtained by substituting the parameters of the used robot model for (3) is passing through the leg's basic position $\boldsymbol{c}_i$, and is very near the line connecting the points on the x axis and y axis with the zero stability margin. If the turning center is on the torso side of this line, the stability margin of the rotation gait is never smaller than zero. This line can be thus used as the border to select the rotation gait. If the turning center is on the outside of the line against the torso, the crawl gait is preferable. Depending on the walking direction angle, select one crawl gait from X-crawl, RX-crawl, Y-crawl, and RY-crawl. In contrast to the above-proposed technique, a geometric construction has been proposed to provide an approximate answer to gait selection [11], where a similar gait-transition technique as in [6] was used.

After selecting the used gait pattern from the position of the turning center, then give the time phase t_i for each leg corresponding to the selected gait. $t_i = 0$ is for the start of the legs' swinging, and $t_i = T_{\rm sw}$ is for its end.

B. Derivation of Leg's Landing Position and Leg's Lifting Position

The landing position of the swinging leg and the lifting position of the supporting leg can be derived from the rotation speed, whose maximum value is determined by the position of the turning center, the selected gait, and the legs' reachable ranges. In this paper, we assume that the reachable ranges of the legs are symmetric about the COG and rectangles for simplicity, as shown in Figs. 2 and 3. The scheme proposed in this paper, however, can also be used for any shape of reachable range of legs.

1) Maximum Rotation Speed: We derive the maximum rotation speed from the position of the turning center and the legs' reachable ranges. From the constraint that the trajectories of the supporting legs must pass through the basic positions of the legs in order for the feet to have common positions in the transition from one gait to another, we can have the curvature radius r_i given by

$$r_i = ||\boldsymbol{c}_i - \boldsymbol{Q}||. \tag{4}$$

As shown in Fig. 7, the basic position of each leg, $\boldsymbol{c}_i$, can be described by the inclining angle ϕ_{ci}. It is given by

$$\phi_{ci} = \mathrm{atan2}\left((c_{iy} - Q_y), (c_{ix} - Q_x)\right). \tag{5}$$

If we set the intersection of the trajectory of the supporting leg and the boundary of the reachable range as $\boldsymbol{p}_{fi}$ for the walking direction, and $\boldsymbol{p}_{ri}$ for the antiwalking direction, we can have the inclining angles corresponding to $\boldsymbol{p}_{fi}$ and $\boldsymbol{p}_{ri}$ as

$$\phi_{fi} = \mathrm{atan2}\left((p_{fiy} - Q_y), (p_{fix} - Q_x)\right) \tag{6}$$

$$\phi_{ri} = \mathrm{atan2}\left((p_{riy} - Q_y), (p_{rix} - Q_x)\right). \tag{7}$$

In order to derive the trajectories of the supporting legs that make the feet have the common positions before and after the gait transition, we introduce the trajectory-partition coefficients K_{qfi} and K_{qri}. These two coefficients are the coefficients that divide the trajectories corresponding to the gait, and use the values listed in Table I. Fig. 8 shows an example of how the trajectory-partition coefficients K_{qfi} and K_{qri} of the X-crawl gait are obtained. Therein, $K_{qf1} = K_{qf4} = 0.5$, $K_{qr1} = K_{qr4} = 0.25$, $K_{qf2} = K_{qf3} = 0.25$, and $K_{qr2} = K_{qr3} = 0.5$ are for dividing the trajectory of each leg to the corresponding part.

Using K_{qfi} and K_{qri}, we can have

$$\theta_{fi} = \frac{|\phi_{fi} - \phi_{ci}|}{K_{qfi}}, \quad \theta_{ri} = \frac{|\phi_{ri} - \phi_{ci}|}{K_{qri}}. \tag{8}$$

Among all of θ_{fi} and θ_{ri}, the smallest one is the feasible maximum rotation angle $\theta_{\max}$, and $\theta_{\max}/T$ is the feasible maximum rotation speed $\dot{\theta}_{\max}$. That is, we can have the maximum rotation speed $\dot{\theta}_{\max}$ given by

$$\theta_{\max} = \min\{\theta_{fi}, \theta_{ri} | i = 1, 2, 3, 4\} \tag{9}$$

$$\dot{\theta}_{\max} = \frac{\theta_{\max}}{T} \tag{10}$$

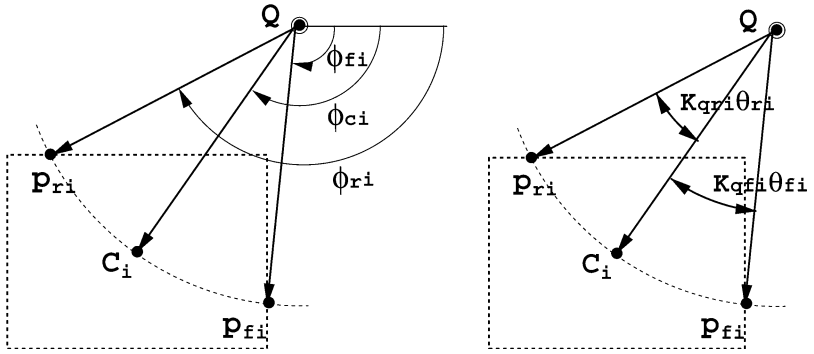

Fig. 7. Reachable angles of a leg around curvature center.

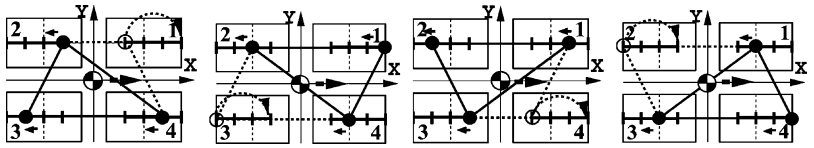

Fig. 8. X-crawl gait to show how the value of K_{qfi} and that of K_{qri} are obtained. Legs 1 and 4 use the front 4/3 part in their reachable range, but legs 2 and 3 use the rear 4/3 part of the trajectories. Counting from the leg's basic position $\boldsymbol{c}_i$, we have the coefficient K_{qfi} in the walking direction where $K_{qf1} = K_{qf4} = 2/4$ and $K_{qf2} = K_{qf3} = 1/4$, and the coefficient K_{qri} in the antiwalking direction where $K_{qr1} = K_{qr4} = 1/4$ and $K_{qr2} = K_{qr3} = 2/4$.

TABLE I
PARTITION COEFFICIENT FOR EACH WALKING PATTERN

X-crawl

leg i	K_{qfi}	K_{qri}
1, 4	0.5	0.25
2, 3	0.25	0.5

RX-crawl

leg i	K_{qfi}	K_{qri}
1, 4	0.25	0.5
2, 3	0.5	0.25

Y-crawl

leg i	K_{qfi}	K_{qri}
1, 2	0.5	0.25
3, 4	0.25	0.5

RY-crawl

leg i	K_{qfi}	K_{qri}
1, 2	0.25	0.5
3, 4	0.5	0.25

O(RO)-rotation

leg i	K_{qfi}	K_{qri}
1, 2, 3, 4	0.5	0.25

where T is the time of one cycle in four steps.

2) Landing Position of the Swinging Leg: The start position of the swinging leg $\boldsymbol{p}_{si}$ is the leg's position at $t_i = 0$, and its end position $\boldsymbol{p}_{ei}$ is the leg's position at $t_i = T_{\rm sw}$. The inclining angle of the landing position of the swinging leg, ϕ_{ei}, is described as

$$\phi_{ei} = \phi_{ci} + K_{qi}\theta \tag{11}$$

through the inclining angle of the legs' basic position ϕ_{ci}, the trajectory-partition coefficient K_{qi} (K_{qfi} or K_{qri}), and the rotation angle θ ($\theta = \dot{\theta}_{in}T$. Therein, $\theta \leq \theta_{\max}$) of one cycle. Note that K_{qi} is K_{qfi} (or K_{qri}) corresponding to θ_{fi} (or θ_{ri}), which is $\min\{\theta_{fi}, \theta_{ri}\}$. For example, if $\theta_{f1} = \min\{\theta_{fi}, \theta_{ri} | i = 1,2,3,4\}$, K_{qf1} must be used. The landing position of the swinging leg, $\boldsymbol{p}_{ei}$, can be thus derived by

$$\boldsymbol{p}_{ei} = \boldsymbol{Q} + \begin{bmatrix} r_i \cos\phi_{ei} \\ r_i \sin\phi_{ei} \\ 0 \end{bmatrix}. \tag{12}$$

3) Lifting Position of the Supporting Leg: The start position of the supporting leg is the landing position of the swinging leg $\boldsymbol{p}_{se}$, and its end position $\boldsymbol{p}_{hi}$ is the leg's position at $t_i = T$. The inclining angle of the supporting leg at the end of supporting phase, ϕ_{hi} can be described as

$$\phi_{hi} = \phi_{ei} - \dot{\theta}(T - T_{\rm sw}) \tag{13}$$

by the inclining angle of the swinging leg at the end of the swinging phase, ϕ_{ei}, and the rotation speed $\dot{\theta}$ ($\dot{\theta} = \dot{\theta}_{in}$. Therein, $\dot{\theta} \leq \dot{\theta}_{\max}$). The lifting position of the supporting leg, $\boldsymbol{p}_{hi}$, is thus given by

$$\boldsymbol{p}_{hi} = \boldsymbol{Q} + \begin{bmatrix} r_i \cos\phi_{hi} \\ r_i \sin\phi_{hi} \\ 0 \end{bmatrix}. \tag{14}$$

C. Planning of Leg Trajectories

The leg trajectory of the swinging leg is a curve connecting its start position $\boldsymbol{p}_{si}$ and its end position $\boldsymbol{p}_{ei}$ with account of height h_{sw}. We use a cos function to define the command position of the swinging leg, $\boldsymbol{p}_{di}$, and its command velocity $\dot{\boldsymbol{p}}_{di}$, as

$$\boldsymbol{p}_{di} = \begin{bmatrix} \frac{p_{six} - p_{eix}}{2} \cos\left(\frac{\pi}{T_{\rm sw}} t_i\right) \\ \frac{p_{siy} - p_{eiy}}{2} \cos\left(\frac{\pi}{T_{\rm sw}} t_i\right) \\ \frac{h_{sw}}{2}\left\{1 - \cos\left(\frac{2\pi}{T_{\rm sw}} t_i\right)\right\} \end{bmatrix} + \frac{1}{2}(\boldsymbol{p}_{si} + \boldsymbol{p}_{ei})$$

$$\dot{\boldsymbol{p}}_{di} = \begin{bmatrix} -\frac{1}{2}(p_{six} - p_{eix})\frac{\pi}{T_{\rm sw}} \sin\left(\frac{\pi}{T_{\rm sw}} t_i\right) \\ -\frac{1}{2}(p_{siy} - p_{eiy})\frac{\pi}{T_{\rm sw}} \sin\left(\frac{\pi}{T_{\rm sw}} t_i\right) \\ h_{sw}\frac{\pi}{T_{\rm sw}} \sin\left(\frac{2\pi}{T_{\rm sw}} t_i\right) \end{bmatrix}.$$

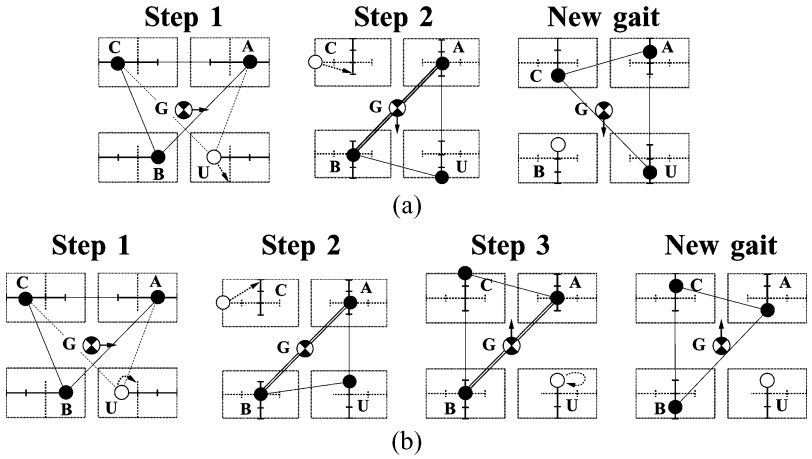

Fig. 9. Gait transition from crawl gait to crawl gait. (a) Case 1. (b) Case 2.

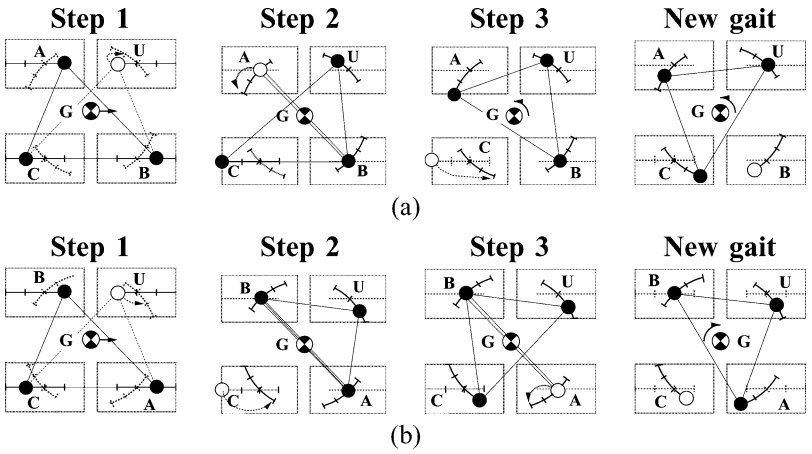

Fig. 10. Gait transition from crawl gait to rotation gait. (a) Case 1. (b) Case 2.

Since the trajectories of the supporting legs are a circle, the command positions of the supporting legs and their command velocities can be given by

$$\boldsymbol{p}_{di} = \boldsymbol{Q} + \begin{bmatrix} r_i \cos\phi_{di} \\ r_i \sin\phi_{di} \\ 0 \end{bmatrix}$$

$$\dot{\boldsymbol{p}}_{di} = \begin{bmatrix} -r_i \sin(\phi_{di})\dot{\phi}_{di} \\ r_i \cos(\phi_{di})\dot{\phi}_{di} \\ 0 \end{bmatrix} = \begin{bmatrix} r_i \sin(\phi_{di})\dot{\theta} \\ -r_i \cos(\phi_{di})\dot{\theta} \\ 0 \end{bmatrix}$$

by the command inclining angle ϕ_{di} defined by

$$\phi_{di} = \phi_{ei} - \dot{\theta}(t_i - T_{\mathrm{sw}}). \tag{15}$$

Through tracking the planned legs' trajectories, the robot can walk in any standard gait around any turning center. Note that the straight-line walking can also be easily performed by setting the radius of the turning center a large value (in simulation and experiment, 10^{10} was used).

IV. Successive Gait Transitions

In Section III, we have made the gait transition performed within the fewest steps possible through designing the feet before and after gait transition to have common positions, and through planning the leg trajectories to make the two supporting legs form a diagonal line located at the basic legs' positions at the DTE point. In this section, we assume that the gait transition is executed at one step before the DTE point, and propose the successive gait-transition procedures while changing the turning center.

While the position of the new turning center is given, we first select the corresponding gait and derive the corresponding legs' positions, then move the legs from the current positions to new positions to perform the successive gait transition. The gait transition between the gaits shown in Fig. 5 can be mainly classified to:

- gait transition from crawl to crawl;
- gait transition from crawl to rotation;
- gait transition from rotation to crawl;
- gait transition form rotation to rotation.

Next, we discuss the successive gait-transition procedures that can perform the above four gait transitions stably and continuously with the fewest steps. Note that in Figs. 9–12 "U" describes the swinging leg at step 1, "C" is the leg opposite to leg U, and "B" is the opposite leg of leg A, respectively.

A. Gait-Transition From Crawl to Crawl

The gait transition from crawl to crawl is divided into the following two cases, based on which leg is first swung at the start of gait transition.

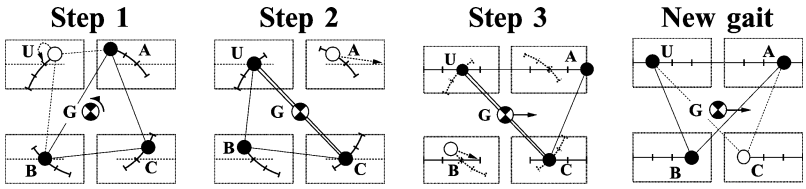

Fig. 11. Gait transition from rotation gait to crawl gait.

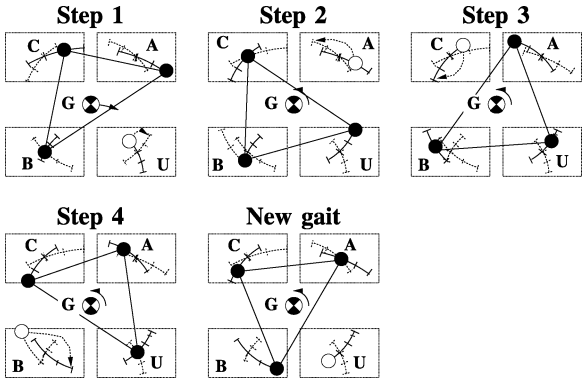

Fig. 12. Gait transition from rotation gait to rotation gait.

Case 1) the front leg is the first swinging leg in the walking direction of the new gait.

Case 2) the back leg is the first swinging leg in the walking direction of the new gait.

The gait transitions for these two cases are shown in Fig. 9. Therein, "A" describes the front leg in the walking direction of the old gait, except for legs U and C.

Step 1 is the state right before the DTE point. The gait transition starts at this step while leg U is first lifted up. Step 2 is at the DTE point. At this step, legs A and B are in the basic legs' positions, and three legs are thus already at the legs' position of the new gait. Since the COG is on the line connecting legs A and B, leg C is possibly swung at this time. Moving leg C to its position of new gait finishes the gait transition. For Cases 1 and 2, the gait transition is performed in this way, but the following difference between Case 1 and Case 2 exists. In Case 1, as shown in Fig. 9(a), since the polygon of supporting legs is formed in the walking direction, the gait transition can be performed successively without stopping the torso. In Case 2, as shown in Fig. 9(b), however, the polygon of supporting legs is not formed in the walking direction. The torso must stop in one step in order for the polygon of supporting legs to be generated in the walking direction.

B. Gait Transition From Crawl to Rotation

Depending on the leg's position at Step 2 of gait transition, we can divide the gait transition from crawl to rotation in two cases, as shown in Fig. 10. Therein, "A" describes the leg swung right after leg U of the new gait.

Step 1 is the state just before the DTE point, and the gait transition starts at this step while leg U is first lifted up. The following two cases, for the gait transition from crawl to rotation, depends on whether leg A can be lifted up or not while shifting from Step 1 to Step 2.

1) Case 1: As shown in Fig. 10(a), leg A is possibly lifted up at Step 2, and can be moved to the new leg position. Leg B is in the basic leg's position at this moment, and still at the leg position of the new gait. At Step 2, in order to guarantee leg C within its reachable range, the torso must stop in one step. After that, leg C is moved to the position of the new gait at Step 3, and the gait transition is finished.

2) Case 2: As shown in Fig. 10(b), since leg A can not be lifted up at the moment of Step 2, leg C is thus moved to the position of the new gait. At this step, since the COG is on the line connecting legs A and B, leg C is possibly swung. Leg A is possibly lifted up at Step 3, thus moving leg A to the position of the new gait and finishing the gait transition. The same as Case 1, leg B is on the basic leg's position at Step 2, and still at the leg position of the new gait. Since leg C is moved to the limit point of the new gait to make leg A possibly move at Step 3, the torso must stop in two steps, Steps 2 and 3. At this point, the same result as that of the standing-posture transformation gait [6] is obtained.

C. Gait Transition From Rotation to Crawl

The gait transition from rotation to crawl can be perform from any state of the rotation gait. Its procedure is shown in Fig. 11. Therein, "A" describes the front leg in the walking direction of new gait, except for legs U and C.

Since leg U is possibly lifted up at Step 1, move leg U to the basic leg position and start the gait transition. While leg U is moved to the basic leg position, leg C is also at the basic leg position. At the start moment of Step 2, the COG is on the line connecting legs U and C. Legs A and B are thus possibly lifted up. At Step 2, leg A is moved to the position of new gait while stopping the torso motion. At Step 3, move leg B to the position of new gait and finish the gait transition. The reason for first swinging leg A instead of leg B is to form a triangle of supporting legs in the walking direction of the new gait.

D. Gait Transition From Rotation to Rotation

Same as the gait transition from rotation to crawl, the gait transition from rotation to rotation can be performed from any state of the rotation gait. Its procedure is shown in Fig. 12. Therein, "A" describes the same leg as in Fig. 10.

The gait transition from rotation to rotation can be easily performed by moving the legs to the position of the new gait one by one.

In addition to the above gait-transition procedures, we add the rule, "the swinging motion of the leg is omitted if the lifting position and the landing position of the leg are same" to shorten the gait-transition time. For comparison, we listed the time of each gait transition in Table II. From the result, it is known that Case 1

TABLE II
COMPARISON OF GAIT-TRANSITION TIME

$\mapsto$	X		RX		Y		RY		O		RO	
Case	1	2	1	2	1	2	1	2	1	2	1	2
X	1/2T	—	—	3/4T	1/2T	3/4T	1/2T	3/4T	3/4T	3/4T	3/4T	3/4T
RX	—	3/4T	1/2T	—	1/2T	3/4T	1/2T	3/4T	3/4T	3/4T	3/4T	3/4T
Y	1/2T	3/4T	1/2T	3/4T	1/2T	—	—	3/4T	3/4T	3/4T	3/4T	3/4T
RY	1/2T	3/4T	1/2T	3/4T	—	3/4T	1/2T	—	3/4T	3/4T	3/4T	3/4T
O	3/4T		3/4T		3/4T		3/4T		T		T	
RO	3/4T		3/4T		3/4T		3/4T		T		T	

Note: X, RX, Y, RY, O, and RO is each gait pattern shown in Fig. 5.

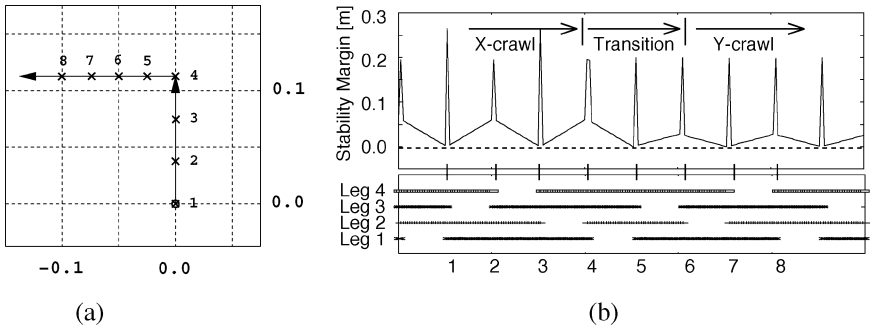

Fig. 13. Walking path of COG, corresponding stability margin, and legs' state for the gait transition from crawl gait to crawl gait (Case 1). (a) Walking path. (b) Stability margin and legs' state.

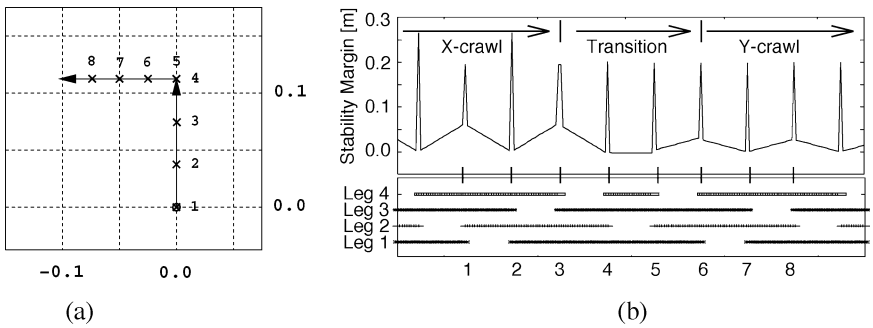

Fig. 14. Walking path of COG, corresponding stability margin, and legs' state for the gait transition from crawl gait to crawl gait (Case 2). (a) Walking path. (b) Stability margin and legs' state.

of the gait transition from crawl to crawl takes the shortest time. Even though the gait transition from rotation to rotation takes the longest time, the torso starts the motion around a new turning center together with the gait transition, and the walking direction is continuously and quickly changed to a new one. Therefore, even the stop of the torso in one or two steps is necessary, and the gait transition can be performed continuously. Note that a shorter time is required than that shown in Table II for the case where the leg has the same lifting/landing positions.

V. SIMULATIONS AND EXPERIMENTS

To verify the validity of the proposed omni-directional static walking algorithm, the computer simulations and the walking experiments by the robot model TITAN-VIII [12] were performed. The robot controller (planning of the gait and the legs' trajectories, the legs' path-tracking control) is built at a PC/AT (Intel MMX Pentium 200 MHz, DRAM: 64 MB) by RTLinux, and the leg trajectories are tracked by resolved motion rate control [13]. The time of swinging leg is fixed at 1.0 [s], and the reachable region is a 0.30 [m] $\times$ 0.20 [m] rectangular region centered at each basic leg's position.

We first show, by computer simulation, the motion trajectory of the torso, the corresponding stability margin, and the supporting/swinging phase of each leg for each gait-transition pattern in Figs. 13–18. Therein, (a) is the motion trajectories of the robot's COG, and (b) is the corresponding stability margin and the legs' state where lines describe the supporting phase of the legs. The numbers 1$\sim$8 in (b) indicate the corresponding points on the trajectories in (a). In Figs. 13–16, the COG of the torso tracks the same trajectories, but the results for different gait transitions are shown. From the results, it is known that the COG of the robot (or torso) moves along line trajectories without sideways motion. It must be more efficient in energy consumption than the case where the robot moves in cooperation with sideways motion. It is also known that the stability margin is always larger than zero for each gait and gait transition. The gait transitions are performed stably. Note that, since the standard gaits were planned on basis of the basic legs' positions, the stability margin is zero at all times if the robot walks along the direction

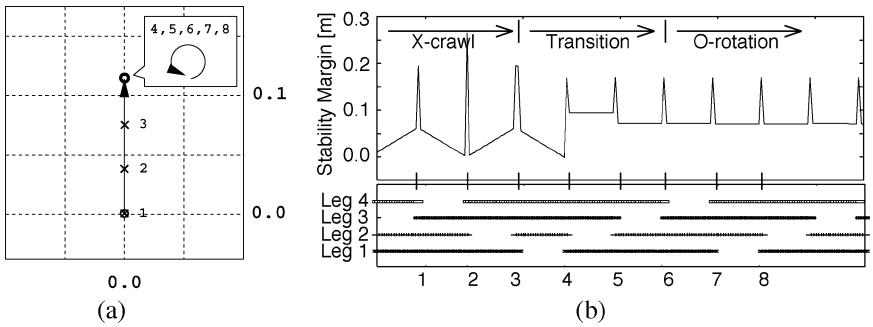

Fig. 15. Walking path of COG, corresponding stability margin, and legs' state for the gait transition from crawl gait to rotation gait (Case 1). (a) Walking path. (b) Stability margin and legs' state.

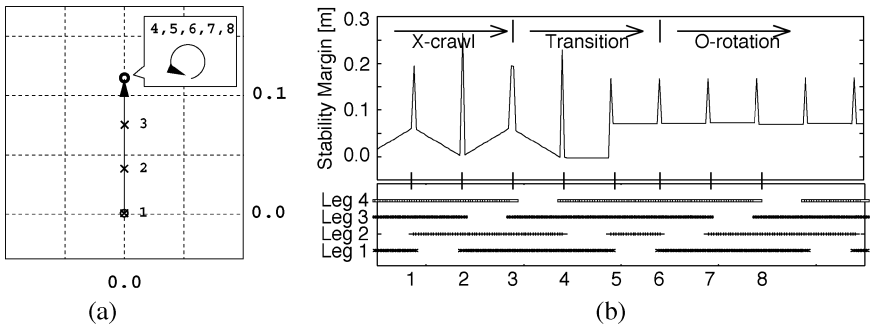

Fig. 16. Walking path of COG, corresponding stability margin, and legs' state for the gait transition from crawl gait to rotation gait (Case 2). (a) Walking path. (b) Stability margin and legs' state.

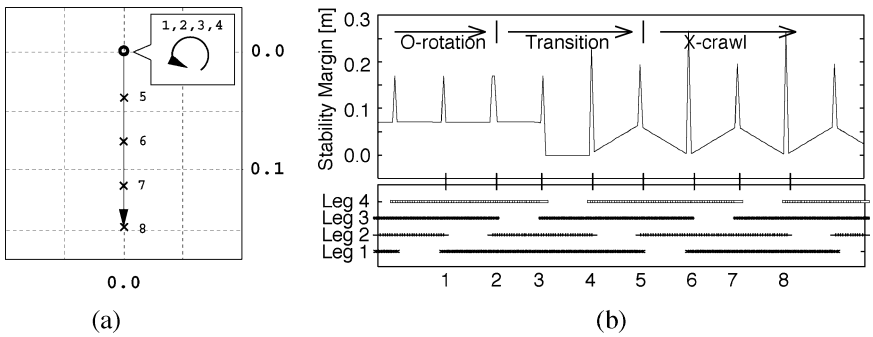

Fig. 17. Walking path of COG, corresponding stability margin, and legs' state for the gait transition from rotation gait to crawl gait. (a) Walking path. (b) Stability margin and legs' state.

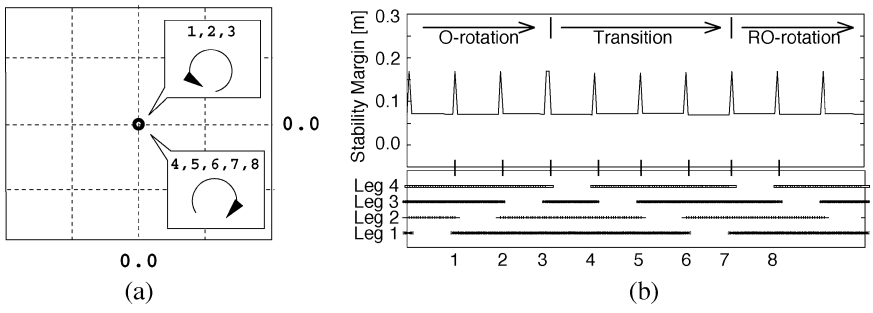

Fig. 18. Walking path of COG, corresponding stability margin, and legs' state for the gait transition from rotation gait to rotation gait. (a) Walking path. (b) Stability margin and legs' state.

of the diagonal line of the basic legs' positions. This problem can be solved by selecting the X-crawl gait and rotation gait as frequently as possible, but not the crawl gait along the diagonal line.

Next, we performed the following experiments:

- walking by each standard gait (forward/backward, left/right, left/right turn, left/right rotation, and straight-line walking with an angle);
- gait transition (crawl→crawl, crawl→rotation, rotation→crawl, and rotation→rotation);

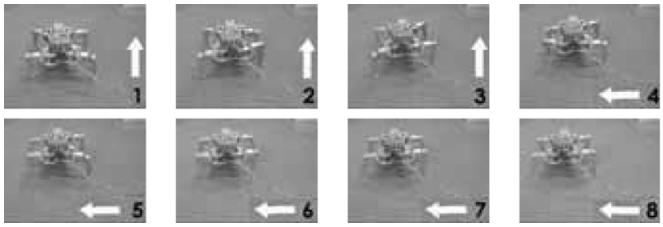

Fig. 19. Photographs to show robot motion for the gait transition from crawl gait to crawl gait (Case 1).

- walking along a figure "8" character.

In the walking experiment of the standard gaits, the robot walked stably. Each gait transition was also checked by the experiment. Fig. 19 shows one example of the gait transition from crawl to crawl. The numbers of the photographs in Fig. 19 is same as that in Fig. 13. The robot is walking forward by the X-crawl gait in 1, 2, and 3, at 4 the left-forward leg starts swinging toward the left, and the gait transition starts. At 5, the right-back leg swings to the left and lands at 6 to finish the gait transition. The robot walks left by the Y-crawl gait in 6, 7, and 8.

From the gait-transition experiments, we know that the robot totally walked stably as the simulation. At Step 2 of the gait transition, in Case 2 from crawl to crawl and in Case 2 from crawl to rotation, however, the torso leaned occasionally. This is because the COG is on the diagonal line at the case, and torso leaning is caused by the difference of the COG between the real and simulation models. Calibrating the parameters of the robot can solve the problem somewhat.

For the experiment walking along a figure "8" character, the robot walks only by the X-crawl gait, and its walking direction is changed through the rotation gait, thus is always stable. As a result, we can conclude that the omnidirectional static walking of the quadruped robot can be well generated by the proposed algorithm.

VI. Conclusion

In this paper, we proposed a successive gait-transition method for a quadruped robot to realize omnidirectional static walking. Experimental tests were executed to show that the omnidirectional static walking of the quadruped robot is possibly generated for most cases. The gait transition was successively performed among the crawl gait and the rotation gait, while the feet held in common position before and after gait transition. The transition time of the gaits was reduced through carefully designing the foot position of the crawl and rotation gaits while limiting the feet in rectangular reachable motion ranges.

References

[1] S. Hirose, "A study of design and control of a quadruped walking vehicle," *Int. J. Robot. Res.*, vol. 3, no. 2, pp. 113–133, 1984.
[2] R. B. McGhee, "Some finite state aspects of legged locomotion," *Math. Biosci.*, vol. 2, pp. 67–84, 1968.
[3] R. B. McGhee and A. A. Frank, "On the stability properties of quadruped creeping gaits," *Math. Biosci.*, vol. 3, pp. 331–351, 1968.
[4] S. Hirose, Y. Fukuda, and H. Kikuchi, "The gait control system of a quadruped walking vehicle," *Adv. Robot.*, vol. 1, no. 4, pp. 289–323, 1986.
[5] S. Hirose, H. Kikuchi, and Y. Umetani, "Standard circular gait of a quadruped walking vehicle," *Adv. Robot.*, vol. 1, no. 2, pp. 143–164, 1986.
[6] S. Hirose and K. Yokoi, "The standing posture transformation gait of a quadruped walking vehicle," *Adv. Robot.*, vol. 2, no. 4, pp. 345–359, 1988.
[7] H. Adachi, N. Koyachi, T. Arai, K. Homma, Y. Shinohara, and K. Nishimura, "Semi-autonomous walking based on leg transition at the border of the leg work space" (in Japanese), *J. Robot. Soc. Japan*, vol. 16, no. 3, pp. 329–336, 1998.
[8] V. Hugel and P. Blazevic, "Toward efficient implantation of quadruped gaits with duty factor of 0.75," in *Proc. IEEE Int. Conf. Robot. Autom.*, Detroit, MI, May 1999, pp. 2360–2365.
[9] J. Bruce, S. Lenser, and M. Veloso, "Fast parametric transitions for smooth quadrupedal motion," in *RoboCup-2001: The Fifth RoboCup Competitions and Conferences*, A. Birk, S. Coradeschi, and S. Tadokoro, Eds. Berlin, Germany: Springer-Verlag, 2002.
[10] S. Hirose and O. Kunieda, "Generalized standard foot trajectory for a quadruped walking vehicle," *Int. J. Robot. Res.*, vol. 10, no. 1, pp. 3–11, 1991.
[11] S. Chitta and J. P. Ostrowski, "New insights into quasi-static and dynamic omnidirectional quadrupedal walking," in *Proc. IEEE/RSJ Int. Conf. Intell. Robots, Syst.*, vol. 4, Maui, HI, Oct. 2001, pp. 2306–2311.
[12] K. Arikawa and S. Hirose, "Development of quadruped walking robot TITAN-VIII," in *Proc. IEEE/RSJ Int. Conf. Intell. Robots, Syst.*, Osaka, Japan, Nov. 1996, pp. 208–214.
[13] D. Whiteney, "Resolved motion rate control of manipulators and human prosthese," *IEEE Trans. Man-Mach. Syst.*, vol. MMS-10, pp. 47–53, Jan. 1969.

Shugen Ma (S'89–M'91) received the B.Eng degree in mechanical engineering from the Hebei Institute of Technology, Tianjin, China, in 1984, and the M.Eng. and Dr.Eng. degrees in mechanical engineering science from the Tokyo Institute of Technology, Tokyo, Japan, in 1988 and 1991, respectively.

From 1991 to 1992, he was with Komatsu Ltd. as a Research Engineer, and from 1992 to 1993, he was with the University of California, Riverside, as a Visiting Scholar. Since July 1993, he has been with the Faculty of Engineering, Ibaraki University, Ibaraki, Japan, where he is currently an Associate Professor. He also holds a Professor position with the Shenyang Institute of Automation, Chinese Academy of Sciences, Shenyang, China. His research interest is in the design and control theory of new types of robots and biorobotics.

Dr. Ma was awarded the Outstanding Paper Prize from SICE in 1992. He is a member of the JSME, SICE, and the Robotics Society of Japan.

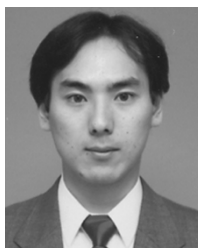

Takashi Tomiyama received the B.Eng. and M.Eng. degrees in systems engineering from Ibaraki University, Ibaraki, Japan, in 1999 and 2001, respectively.

In April 2001, he joined Toshiba Tec Corporation, Tokyo, Japan. His research interest is control of walking robots.

Mr. Tomiyama is a member of the Robotics Society of Japan.

Hideyuki Wada received the B.Eng. degree in systems engineering from Ibaraki University, Ibaraki, Japan, in 2001.

In April 2001, he joined System Technology Corporation, Tokyo, Japan. His research interest is control of walking robots.